ACCOUNTS
of chemical research

Colloidal Chemical Synthesis and Formation Kinetics of Uniformly Sized Nanocrystals of Metals, Oxides, and Chalcogenides

SOON GU KWON AND TAEGHWAN HYEON*

National Creative Research Initiative Center for Oxide Nanocrystalline Materials and School of Chemical and Biological Engineering, Seoul National University, Seoul 151-744, Korea

RECEIVED ON FEBRUARY 20, 2008

CONSPECTUS

Nanocrystals exhibit interesting electrical, optical, magnetic, and chemical properties not achieved by their bulk counterparts. Consequently, to fully exploit the potential of nanocrystals, the synthesis of nanocrystals must focus on producing materials with uniform size and shape. Top-down physical processes can produce large quantities of nanocrystals, but controlling the size is difficult with these methods. On the other hand, colloidal chemical synthetic methods can produce uniform nanocrystals with a controlled particle size. In this Account, we present our synthesis of uniform nanocrystals of various shapes and materials, and we discuss the kinetics of nanocrystal formation.

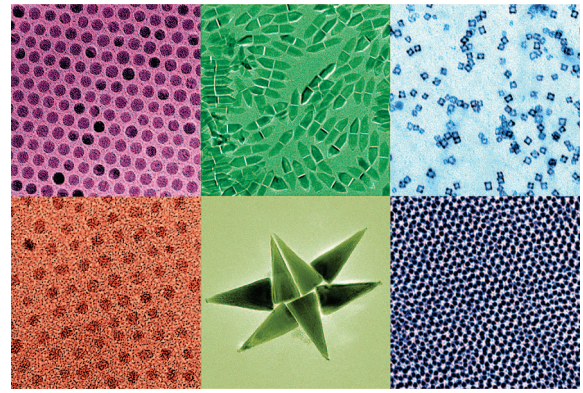

We employed four different synthetic approaches including thermal decomposition, nonhydrolytic sol−gel reactions, thermal reduction, and use of reactive chalcogen reagents. We synthesized uniform oxide nanocrystals via heat-up methods. This method involved slowly heat-up reaction mixtures composed of metal precursors, surfactants, and solvents from room temperature to high temperature. We then held reaction mixtures at an aging temperature for a few minutes to a few hours. Kinetics studies revealed a three-step mechanism for the synthesis of nanocrystals through the heat-up method with size distribution control. First, as metal precursors thermally decompose, monomers accumulate. At the aging temperature, burst nucleation occurs rapidly; at the end of this second phase, nucleation stops, but continued diffusion-controlled growth leads to size focusing to produce uniform nanocrystals.

We used nonhydrolytic sol−gel reactions to synthesize various transition metal oxide nanocrystals. We employed ester elimination reactions for the synthesis of ZnO and TiO_2 nanocrystals.

Uniform Pd nanoparticles were synthesized via a thermal reduction reaction induced by heating up a mixture of $Pd(acac)_2$, tri-*n*-octylphosphine, and oleylamine to the aging temperature. Similarly, we synthesized nanoparticles of copper and nickel using metal(II) acetylacetonates. Ni/Pd core/shell nanoparticles were synthesized by simply heating the reaction mixture composed of acetylacetonates of nickel and palladium.

Using alternative chalcogen reagents, we synthesized uniform nanocrystals of various metal chalcogenides. Uniform nanocrystals of PbS, ZnS, CdS, and MnS were obtained by heating reaction mixtures composed of metal chlorides and sulfur dissolved in oleylamine.

In the future, a detailed understanding of nanocrystal formation kinetics and synthetic chemistry will lead to the synthesis of uniform nanocrystals with controlled size, shape, and composition. In particular, the synthesis of uniform nanocrystals of doped materials, core/shell materials, and multicomponent materials is still a challenge. We expect that these uniformly sized nanocrystals will find important applications in areas including information technology, biomedicine, and energy/environmental technology.

Published on the Web 08/06/2008 www.pubs.acs.org/acr
10.1021/ar8000537 CCC: $40.75

I. Introduction

For the last 30 years, the synthesis of nanocrystals with sizes ranging from 1 to 50 nm has been intensively pursued, not only for their fundamental scientific interest, but also for their many technological applications.[1] Nanocrystals exhibit very interesting size-dependent electrical, optical, magnetic, and chemical properties that cannot be achieved by their bulk counterparts. For many future applications, the synthesis of uniformly sized nanocrystals is of key importance, because their physical and chemical properties are strongly dependent on their dimensions, which are broadly referred to as the size effect.[1−3] This size effect has great potential to the designed synthesis of nanocrystals, because the material properties can be tuned by varying the size and shape. Accordingly, the most important requirement in the synthesis of nanocrystals is the good controllability of their size and shape while maintaining their uniformity. In other words, to fully exploit the potential of nanocrystals with the desired properties, it is essential that they be synthesized with uniform size and shape.

There are two different approaches to synthesize nanocrystals: the top-down physical processes and the bottom-up chemical methods. The physical processes can produce large quantities of nanocrystals, whereas the synthesis of uniformly sized nanocrystals and their size-control are very difficult to achieve. On the other hand, colloidal chemical synthetic methods can be used to synthesize uniform nanocrystals with a controlled particle size.[1] Furthermore, various shaped nanocrystals can be synthesized by varying the reaction conditions. In 1993, Murray, Norris, and Bawendi reported the synthesis of uniform cadmium chalcogenide nanocrystals using the so-called "hot injection" method, which is a landmark work in the colloidal chemical synthesis of nanocrystals.[4] The rapid injection of the reactive precursor into the hot coordinating solvent makes the solution highly supersaturated instantaneously. Binding of bulky coordinating solvent molecules to cadmium and chalcogen atoms retards the crystal formation, keeping the supersaturation level high for a while. In such a high supersaturation condition, nucleation and growth of colloidal crystals occur in controlled ways, namely, burst nucleation and size focusing, as discussed in detail below.[4,5] The coordinating molecules bound on the surface of the nanocrystals endow them with good colloidal stability in organic solvents. In the original paper in 1993, the relative standard deviation (σ_r) of the size distribution of the nanocrystals was ~10%, and the synthetic method has since been further improved and is now able to produce CdSe nanocrystals with an σ_r of $\leq$5%.[6]

In devising the synthetic schemes for nanocrystals, we have to consider two aspects: the synthetic chemistry and the formation kinetics of nanocrystals. Needless to say, they are closely related to one another, making it hard to establish a general synthetic method that is widely applicable to various materials. For the last ten years, our research group has been working on the development of reliable synthetic methods for uniformly sized nanocrystals. In this Account, we present some selected results on the synthesis of uniform nanocrystals by our research group. In the following four sections, which are categorized by their synthetic chemistry, we try to present general aspects of the chemistry and kinetics involved in the synthesis of nanocrystals.

II. Synthesis of Uniformly Sized Nanocrystals of Metals and Oxides via Thermal Decomposition Routes

In the hot injection method, the size distribution control is essentially a kinetic process driven by high initial supersaturation. It requires that the precursor be reactive enough to induce high supersaturation immediately upon injection. This hot injection method has been successfully extended to the synthesis of nanocrystals of various materials including magnetic metals and metal oxides.[1] They are highly pursued materials for use in data storage and biomedical applications.[7,8] For example, in 2000, our group reported the synthesis of iron nanocrystals via the hot injection method using $Fe(CO)_5$ and trioctylphosphine oxide (TOPO) as the precursor and the coordinating solvent, respectively.[9] However, the hot injection method has several intrinsic limitations. First of all, a highly reactive precursor is not available for many materials. Second, extremely vigorous reactions at high temperature can become very dangerous. Third, it is not easy to adapt this method for the large scale synthesis of uniformly sized nanocrystals because it is very difficult to keep a uniform temperature profile in a large-scale reactor. Consequently, we tried to develop a new reliable method of synthesizing uniform nanocrystals.

In 2001, we reported a modified version of the synthetic method we developed in 2000.[10] In a typical synthesis, a reaction solution containing $Fe(CO)_5$, oleic acid, and dioctyl ether is prepared and is slowly heated to reflux. The initial product is uniformly sized, poorly crystalline iron nanoparticles, which are converted to iron oxide nanocrystals while maintaining their size and uniformity by reacting them with a

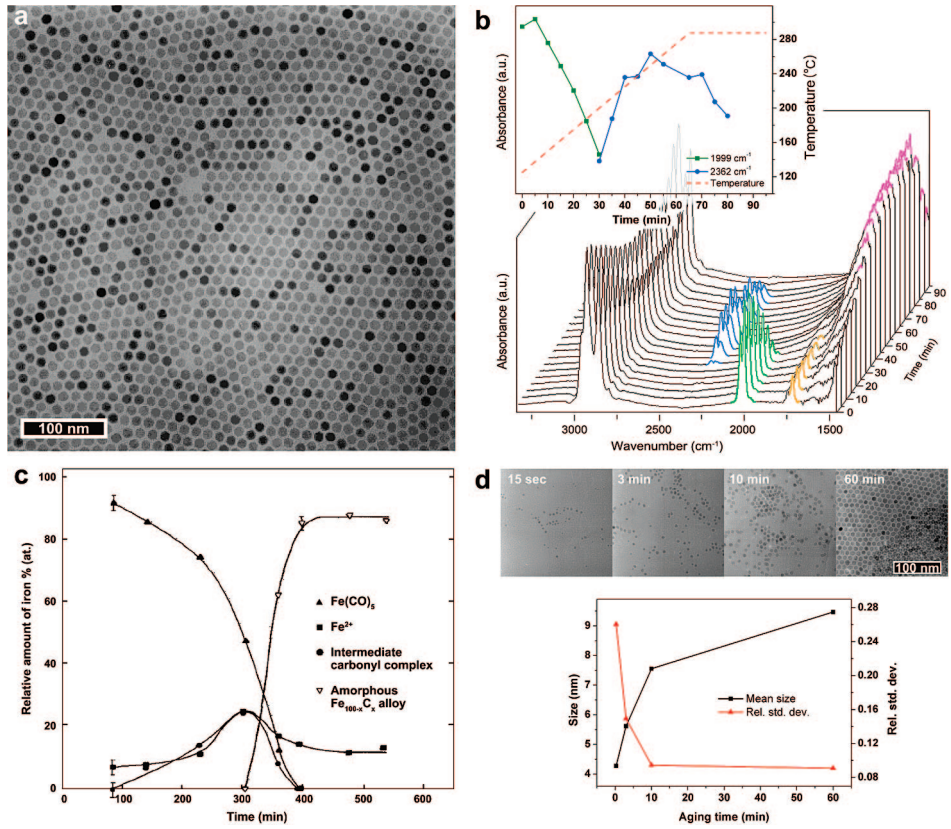

FIGURE 1. (a) TEM image of iron oxide nanocrystals. (b) In situ IR spectroscopy data presented in 3D and 2D plots. The peaks indicated as blue (2362 and 2339 cm^{-1}), green (2023 and 1999 cm^{-1}), orange (1713 cm^{-1}), and magenta (1590−1520 cm^{-1}) are assigned to CO_2, carbonyl ligand in $Fe(CO)_5$, C═O bond in free oleic acid, and metal binding carboxylate group, respectively. (c) Temporal changes of the relative amount of various Fe species in the reaction solution initially containing $Fe(CO)_5$, oleoyl sarcosine, and decalin under reflux condition. Reprinted from 12, Copyright 1988, with permission from Elsevier. (d) TEM images of iron oxide nanocrystals sampled during the heating procedure and their temporal change of the size distribution. Aging time is set as zero when the solution just reached the aging temperature.

mild chemical oxidant, trimethylamine *N*-oxide [$(CH_3)_3NO$]. The iron oxide nanocrystals are in a mixed phase of γ-Fe_2O_3 and Fe_3O_4.[11] Interestingly, this simple heat-up method produced highly uniformly sized nanocrystals without external operation for the size distribution control (Figure 1a).

Fe^0 atoms generated from the thermal decomposition of $Fe(CO)_5$ are transformed to polynuclear iron clusters, which in turn lead to the nucleation and growth of iron nanocrystals.[12] In our hot injection method reported in 2000, the decomposition of $Fe(CO)_5$ and the formation of iron nanoparticles occur almost instantaneously upon injection. On the other hand, in the modified method with slow heating, there is an intermediate step between the decomposition of $Fe(CO)_5$ and the formation of iron nanoparticles. In this intermediate step, oleic acid molecules coordinate to Fe atoms, and some coordinated oleic acid molecules seem to decompose to generate CO_2, as shown in the infrared (IR) spectra in Figure 1b. The Mössbauer spectroscopic data reported by another research group also showed that Fe^{2+} and unidentified iron carbonyl compounds appeared and accumulated transiently in the intermediate step (Figure 1c).[12] The presence of the intermediate step suggests that the coordination of oleic acid stabilizes large iron complexes. It was reported that the presence of carboxylic acid in the solution retarded the formation of iron nanoparticles from the thermal decomposition of $Fe(CO)_5$.[13] The nucleation reaction in a homogeneous solution has a high energy barrier, as is discussed below. As a result, the stabilization of the intermediate iron complexes delays the nucleation process and, consequently, these intermediate species accumulate in the solution. Following the intermediate step, the nucleation and growth processes start suddenly. As shown in Figure 1d, the temporal change of the nanoparticle size distribution was almost terminated within 10 min of the start of the nucleation, during which time the increase of the mean size and the decrease of σ_r occurred simultaneously.

Although the exact size distribution control mechanism of this method has not been completely elucidated yet, the following general remarks can be made. First, the presence of oleic acid results in the extension of the intermediate step at high temperature. Second, this intermediate step is closely related to the size distribution control in the heat-up method. In controlled experiments using amines as the surfactant, which catalyze the decomposition of $Fe(CO)_5$, there is no intermediate step, and this results in uncontrolled growth, producing polydisperse iron particles. Inspired by these results, we generalized our heat-up method to synthesize nanocrystals of cobalt ferrite and manganese ferrite having a uniform size distribution.[14,15] In both cases, the thermal decomposition of the metal complexes in the presence of oleic acid produces uniform cobalt−iron and manganese−iron alloy nanoparticles, which are oxidized to the final ferrite nanocrystals by reacting them with $(CH_3)_3NO$. Furthermore, our group achieved the 1-nm-level size-controlled synthesis of monodisperse iron oxide nanocrystals by combining the heat-up and seed-mediated growth methods.[11]

Our original heat-up method had some room for improvement. According to the results discussed above, the presence of thermally stable intermediate species, rather than the use of the thermally labile precursor, is essential for the size distribution control of the nanocrystals in the heat-up method. This result allows us a much wider choice of precursors, including metal salts, which are easier to handle and much cheaper than organometallic precursors. In 2004, we reported the synthesis of uniform metal oxide nanocrystals via the heat-up method using metal−oleate complexes as the precursors.[16] We chose these metal salts based on the observation that an iron−oleic acid complex is generated in situ in the intermediate step of our previous heat-up method. Metal−oleate complexes are easily prepared from the reaction between metal chlorides and sodium oleate. In a typical synthesis, metal−oleate complex solution ([metal] = 0.25 M) was slowly heated to temperatures near 300 °C or higher, yielding highly uniform nanocrystals. The crystallization yield, which is defined as the ratio of the amount of metal in the form of nanocrystals to the total amount of metal in the reaction mixture solution, is 0.94 in the synthesis of iron oxide nanocrystals. This modified heat-up method has been applied to the synthesis of uniform nanocrystals of various materials such as hexagonal-cone-shaped ZnO and pencil-shaped CoO (Figure 2).[17,18] Especially, iron oxide nanocrystals synthesized via this method show remarkable size uniformity with a σ_r of less than 5% in the best case. The controllability over both the mean size and the size uniformity was clearly demonstrated with the size dependence of the magnetic property of the synthesized iron oxide nanocrystals, as shown in Figure 3. Because of its simplicity, the heat-up method using a metal−oleate precursor is highly advantageous for scale-up, as demonstrated by the production of iron oxide nanocrystals in tenths of grams from a single batch reaction without the deterioration of the size uniformity. Iron nanocrystals can be synthesized by the in situ reduction of Fe ions at reaction temperatures of ≥380 °C.[16,19]

A detailed kinetics study of the synthetic system of iron oxide nanocrystals was carried out to investigate the size distribution control mechanism of the heat-up method. The kinetics of nanocrystal formation was traced by sampling a series of aliquots from the reaction solution during the synthetic procedure at arbitrary time intervals. A detailed description on the experimental techniques used in this study is presented in ref 20. Under heating, carboxylate groups in metal−oleate complexes decompose into CO_2, CO, H_2, and hydrocarbons, which leads to the formation of metal oxide crystals. Notably, as shown in Figure 4a, there was a time lag of about 10 min between the thermal decomposition of the iron−oleate complex and the formation of iron oxide nanocrystals. We think that intermediate polyiron oxo cluster species are generated and accumulated during this time lag. When the solution temperature reached the aging temperature (320 °C), burst nucleation occurred abruptly. After that, the mean size of the nanocrystals increased rapidly in concurrence with the decrease of σ_r, which reached a minimum within 4 min after aging (Figures 4b,c).

The two heat-up processes described above, using $Fe(CO)_5$ or iron−oleate complex as the precursor, have significant similarities in their kinetics. Both have an intermediate step between the disappearance of the precursors and the formation of the nanocrystals. Also, the rapid narrowing of the size distribution and the fast growth of the nanocrystals occur simultaneously. To explain these phenomena, we made a kinetic model for the formation of spherical nanocrystals.[20] The model consists of three processes. In process I, the precursor, P, is converted to the monomer, M, which is the minimal building unit of crystal.

$$P \rightarrow M \quad (1)$$

Process II is the nucleation process in which crystal C is formed from the monomers:

$$xM \rightarrow C_x \quad (2)$$

where C_x is a crystal particle composed of x monomers. In process III, a crystal particle can grow by receiving more monomers from the solution (precipitation) or lose its monomers to

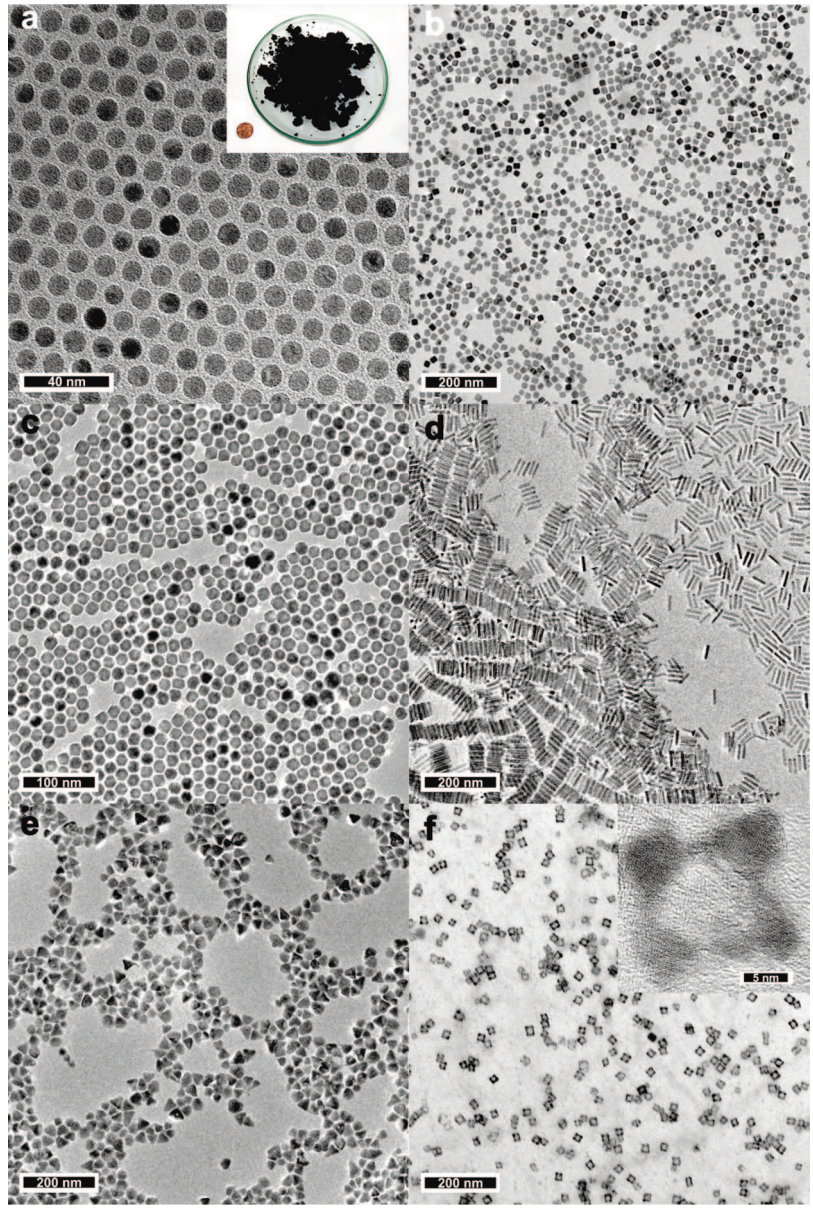

FIGURE 2. TEM images of (a) iron oxide, (b) iron, (c) MnO, (d) CoO, and (e) ZnO nanocrystals and (f) iron nanoframes. In the inset of panel a, iron oxide nanocrystals synthesized in a single-batch reaction are shown. Iron nanoframes in panel f were fabricated via (110)-facet selective etching of iron nanocrystals. Molten salt corrosion induced by sodium ion added seems responsible for the etching process.[19]

the solution (dissolution). It is assumed that the particles are so well dispersed that no agglomeration occurs.

$$C_x + yM \rightleftarrows C_{x+y} \qquad (3)$$

Process II is described by the nucleation rate equation in which the number of nuclei generated per unit time is expressed in the form of the Arrhenius equation.[1] In process III, due to the size dependence of the particle solubility, a spherical particle can grow or dissolve depending not only on the supersaturation of the solution but also on the particle size. Talapin and his colleagues derived a growth rate equation that describes this process.[21] We used these nucleation and growth rate equations and successfully simulated the hot injection process of CdSe nanoparticle synthesis.[1] In the heat-up process, we assumed that the monomers are generated from the thermal decomposition of the precursors. Therefore, the reaction kinetics of the thermal decomposition of iron−oleate complex shown in Figure 4a was used as process I. As shown in the insets of Figure 4b,c, our simulation result based on this assumption reproduced the experimental results quite closely, providing strong evidence for our theoretical model.[20]

As shown in Figure 5a, there are three periods in the simulation of the heat-up process. In the first period, the monomers are generated at the cost of the precursors. Due to the

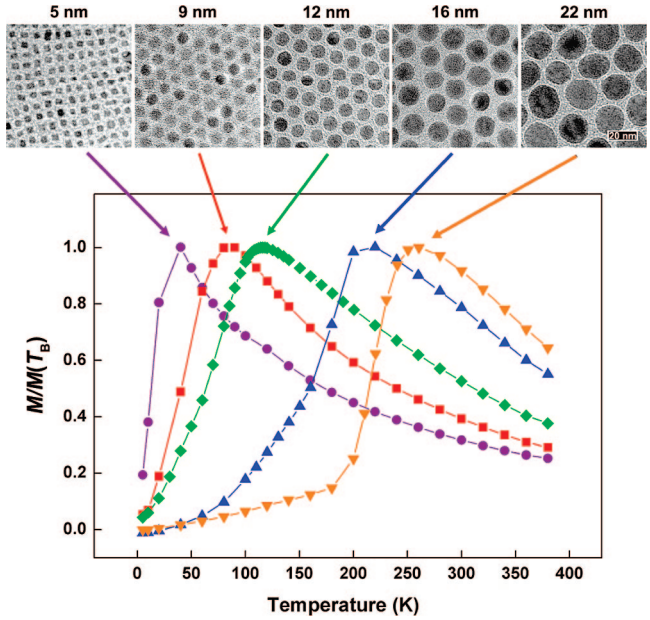

FIGURE 3. Plots for zero-field-cooling magnetization (*M*) of iron oxide nanocrystals of various sizes.[16] TEM images of iron oxide nanocrystals in the samples are shown together with the values of their mean size.

high chemical potential of the nucleus, the nucleation reaction is retarded, and the monomers accumulate during this period. In the second period, the solution is so highly supersaturated with the monomers that the energy barrier for nucleation is overcome. As a result, the fast nucleation of the crystal particles occurs, and the particle number concentration increases abruptly. In concurrence, the rapid consumption of the monomer by the crystal formation leads to a decrease in the supersaturation level. As a result, the smaller, unstable nuclei dissolve back to the monomers during the nucleation process, and only the part of nuclei that are large and stable enough to withstand the decrease of the supersaturation survive at the end of the second period. This process is reflected in Figure 4b as the sharp increase and decrease in the particle number concentration in the first few minutes. After the short burst of nucleation, the nucleation process is stopped by itself because of the monomer consumption, and the third period follows. In the early stage of the third period, however, the supersaturation level is still high enough to keep the particles growing in diffusion-controlled growth mode in which the larger particles grow slower than the smaller ones. The condition of no additional nucleation and diffusion-controlled growth leads to size focusing, in which the rapid narrowing of the size distribution and fast increase in the mean size of the nanoparticles occur simultaneously.[5,21] In the later part of the third stage, the monomers in the solution are almost exhausted. In this condition, the monomers dissolve from the smaller particles and precipitate on the larger particles. This process, which is widely known as the Ostwald ripening, is essentially the same as the process in the second period in which the unstable nuclei dissolve. In the Ostwald ripening process, the larger particles grow faster than the smaller ones, which counteracts the focusing effect. As a result, the size distribution broadens in the later part of the third period.

In summary, the process of size distribution control consists of three steps; the monomer accumulation in the first period, burst nucleation in the second period, and size focusing in the third period. Interestingly, these three steps are well-fitted to the well-known LaMer model, a classical theoretical model for the formation of monodisperse particles.[22] It should be noted that the size focusing effect in the heat-up process is a kinetically driven process, as it is in the case of the hot injection, and the state of the uniform size distribution lasts only for a while, as shown in Figure 4d. The process of size distribution control and the accumulation of the monomers in the simulation results in Figure 5a,b are consistent with the experimental data shown in Figures 1b–d and 4b,c. Consequently, our theoretical work showed that the building-up of a high monomer concentration in the intermediate step is essential for the size distribution control in the heat-up method.

III. Synthesis of Metal Oxide Nanocrystals via Nonhydrolytic Sol–Gel Reactions

Our group has exploited nonhydrolytic sol–gel processes to synthesize various transition metal oxide nanocrystals. In contrast to conventional sol–gel processes, which are based on the hydrolysis and condensation of metal precursors in an aqueous alcohol solvent,[23] the nonhydrolytic sol–gel reaction proceeds by reactions of the metal precursors in organic media.[24] This nonhydrolytic sol–gel process has unique advantages for the synthesis of metal oxide nanocrystals.[25] The reactivity of the precursors can be finely controlled by using various surfactants and solvents. Consequently, uniformly sized and highly crystalline nanocrystals can be synthesized in controllable sizes. By exploiting these advantages, we synthesized highly uniform metal oxide nanocrystals via nonhydrolytic sol–gel routes.

In 2003, we reported the synthesis of uniform ZrO_2 nanocrystals via alkyl halide elimination reaction between zirconium(IV) isopropoxide [$Zr(O^iPr)_4$] and ZrX_4 (X = Cl, Br) in TOPO as a coordinating solvent.[26] The molar ratio of $Zr(O^iPr)_4$ and ZrX_4 is 4:5 and the concentration of Zr is 0.45 mol kg^{-1}. In an alkyl halide elimination reaction, condensation between

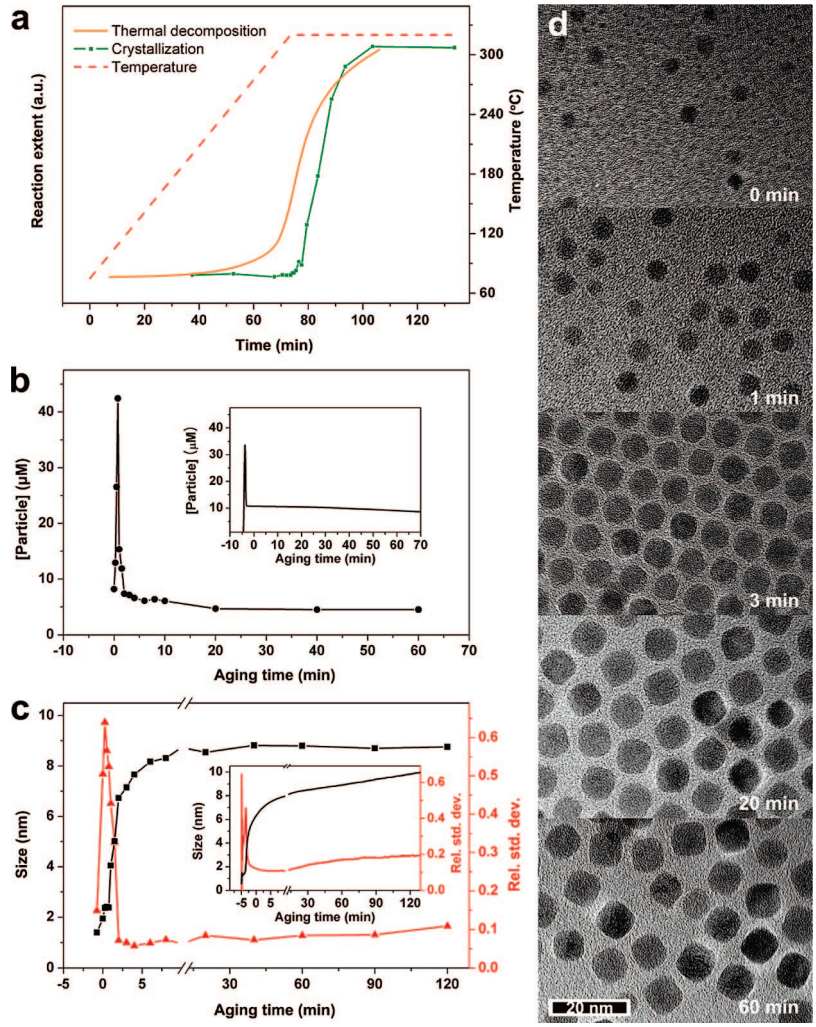

FIGURE 4. (a) Temporal changes of the solution temperature and the reaction extent of the thermal decomposition and the crystallization of nanocrystals during the synthesis of iron oxide nanocrystals, (b, c) temporal changes of the particle number concentration (b) and the mean size and the relative standard deviation of the particle size distribution (c). In the insets, the corresponding parameters from numerical simulation result are shown. Panel d shows TEM images of iron oxide nanocrystals in the samples drawn from the reaction solution at various aging times.

metal alkoxide and metal halide leads to the formation of M−O−M linkages (Scheme 1).[24] This reaction route was confirmed by the separation and identification of isopropyl chloride from the reaction solution, which is the expected byproduct according to Scheme 1. The synthesized ZrO_2 nanocrystals have good size uniformity and are a highly crystalline tetragonal phase (Figure 6a). The precursor solution is prepared at room temperature and slowly heated to and held at the aging temperature of 340 °C. The crystallization yield was measured to be 0.44. As is in the case of the thermal decomposition route, the procedure is easy to scale-up to the multigram scale. Prior to our synthesis of ZrO_2 nanocrystals, Colvin and her colleagues used an alkyl halide elimination reaction to synthesize TiO_2 nanocrystals.[27] They adopted the hot injection method, injecting titanium(IV) alkoxide [$Ti(OR)_4$] into a hot solution containing titanium halide [TiX_4] and TOPO.

It is interesting that the synthetic procedures for TiO_2 and ZrO_2 nanocrystals reported are quite different, although both utilize the same reaction chemistry. This difference reflects the correlation between the synthetic chemistry and the nanocrystal formation kinetics involved. The precursors for ZrO_2 nanocrystals are quite stable compared with those for TiO_2 nanocrystals, and consequently, the former is not suitable for the hot injection method. When we performed the synthesis of ZrO_2 nanocrystals via the hot injection method as a control experiment, an extremely small number of polydisperse nanocrystals were produced. During the synthesis of ZrO_2 nanocrystals

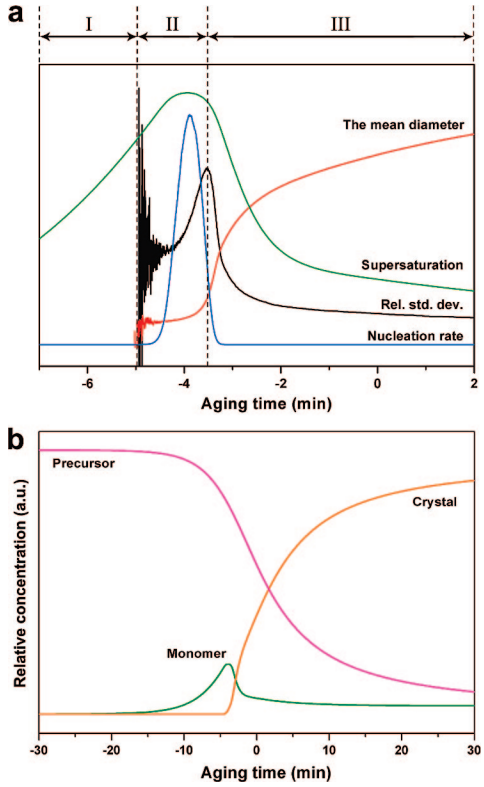

FIGURE 5. Temporal changes of various parameters from the simulation result of the heating process. They are obtained from the same simulation result shown in the insets of Figure 4b,c.

SCHEME 1

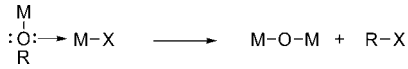

via the heat-up method, we observed that the alkyl halide elimination reaction between $Zr(O^iPr)_4$ and $ZrCl_4$ showed autocatalytic behavior, in which a long induction period precedes the rapid increase in the reaction extent, as shown in Figure 6b. It is very interesting that the overall behavior of the reaction kinetics for the synthesis of ZrO_2 nanocrystals (Figure 6b) is very similar to that of the synthesis of iron oxide nanocrystals via the heat-up method (Figure 4a).

We employed ester elimination reactions for the synthesis of nanocrystals of ZnO and TiO_2.[28,29] As shown in Schemes 2 and 3, these ester elimination reactions result in the formation of metal hydroxide, which is further condensed to form M–O–M linkage. In the synthesis of ZnO nanocrystals, zinc(II) acetate and 1,12-dodecanediol (molar ratio of 1:3–1:6) were used as the precursor and the reactant, respectively (Scheme 2), whereas $Ti(O^iPr)_4$ and oleic acid (molar ratio of 1:3) were used in the synthesis of TiO_2 nanocrystals (Scheme 3). In the synthesis of these two kinds of nanocrystals, the reaction solutions prepared at room temperature are slowly heated to the aging temperatures and aged for a few

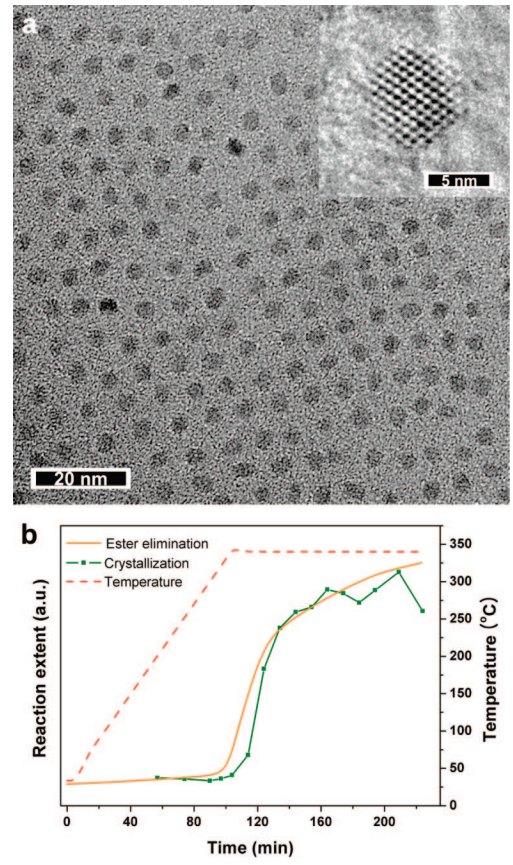

FIGURE 6. (a) TEM image of ZrO_2 nanocrystals and (b) temporal changes of the solution temperature and the reaction extent of ester elimination and the crystallization during the synthesis of ZrO_2 nanocrystals.

SCHEME 2

SCHEME 3

hours. In both cases, the corresponding ester compounds in Schemes 2 and 3 were isolated and identified as the byproducts, confirming the ester elimination reaction pathway. The synthesized ZnO nanocrystals have various shapes including cone, hexagonal cone, and rod shapes (Figure 7a–c). The synthesized TiO_2 nanocrystals exhibited a rod shape with a high aspect ratio (Figure 7d).

During the synthesis of ZnO nanocrystals, the acetate group dissociates steadily as the temperature increases and the formation of ester starts at around 145 °C, as shown in Figure 8a. The reaction solution remains clear and transparent well above 200 °C and then turns to turbid white, indicating the formation of the nanocrystals. A similar pattern has been

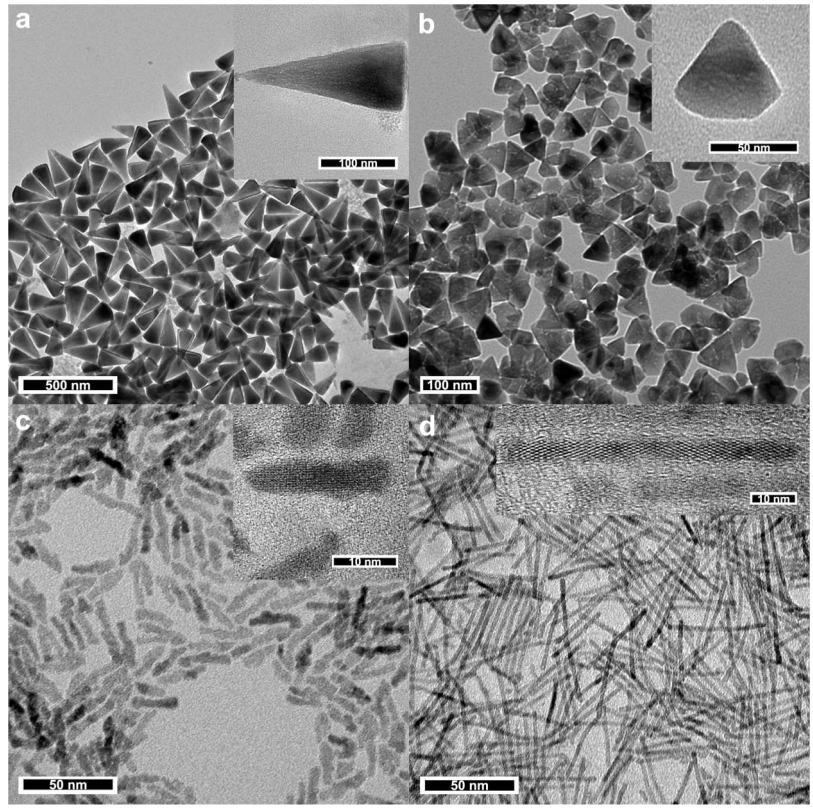

FIGURE 7. (a−c) TEM images of ZnO nanocrystals. They were made in cone (a), hexagonal cone (b), and rod shapes (c) when oleic acid, oleylamine, and tetradecylphosphonic acid were used as the surfactants, respectively. (d) TEM image of TiO_2 nanorods.

observed during the synthesis of TiO_2 nanocrystals. When the reaction mixture composed of oleic acid and $Ti(O^iPr)_4$ was heated at 100 °C, oleate and hydroxyl groups on Ti(IV) complexes were observed, as shown in Figure 8b. However, almost no TiO_2 nanocrystals were generated when the reaction mixture was aged at temperatures below 200 °C. As mentioned above, M−OH, a product of the ester elimination reaction, acts as the monomeric unit for metal oxide nanocrystals. The crystallization yield of TiO_2 nanocrystals is measure to be 0.17. Consequently, during the synthesis of nanocrystals of ZnO and TiO_2 by the heat-up method, the generation of the monomers and the formation of the nanocrystals are temporally separated, which is reminiscent of the three-step model for the synthesis of iron oxide nanocrystals described above.

IV. Synthesis of Nanoparticles of Pd, Cu, and Ni and Ni/Pd Core/Shell Structures via Thermal Reduction Routes

Colloidal nanoparticles of platinum group metals have attracted much attention for their applications to catalysis. The solution-phase reduction of metal ions has been widely employed for the synthesis of colloidal metal nanoparticles. In the conventional Brust method, sodium borohydride was used as the reducing agent. In the polyol method, polyol compounds were used as the reducing agents under heating.

In 2003, we reported the synthesis of uniform palladium nanoparticles (we described them as nanoparticles instead of nanocrystals because of their poor crystallinity).[30] This method uses only two kinds of chemicals, palladium(II) acetylacetonate [$Pd(acac)_2$] as the precursor and tri-*n*-octylphosphine (TOP) and oleylamine as the coordinating solvents. Heating the mixture of $Pd(acac)_2$ and the coordinating solvent ([Pd] = 33 μM) to the aging temperature yields nanoparticles in the size range of 3.5−7 nm depending on the ratio of TOP to oleylamine (Figure 9a). The crystallization yield was measured to be 0.87. There are two interesting points in our synthesis of palladium nanoparticles. First, this method does not use any apparent reducing agent, which greatly simplifies the synthetic procedure. The reduction mechanism has not been clearly elucidated yet. According to the infrared spectra, the coordination of TOP induces a change in the coordination mode of the acetylacetonate group in $Pd(acac)_2$ from η^2 to η^1 (Figure 9b, Scheme 4). It seems that reductive elimination or thermal dissociation of acetylacetonate radicals from the Pd complex under heating conditions might be responsible for the reduc-

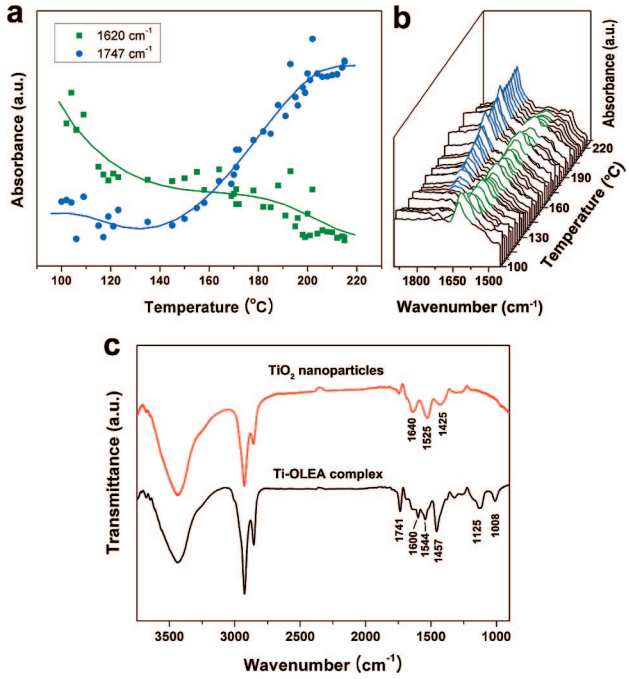

FIGURE 8. (a, b) In situ IR data obtained during the synthesis of ZnO nanocrystals. The heating rate was 2 K/min. The absorption bands in the 1600−1620 cm^{-1} range and at 1747 cm^{-1} are from $Zn(OAc)_2$ and free ester groups, respectively.[28] (c) Fourier transform IR spectra of Ti−oleate complexes and TiO_2 nanocrystals.[29] Absorptions at 1457 and 1544 cm^{-1} are from the carboxylate group coordinated to Ti^{4+}. The peaks at 1600 and 1741 cm^{-1} are from Ti−OH bonding and the carbonyl group in free ester, respectively.

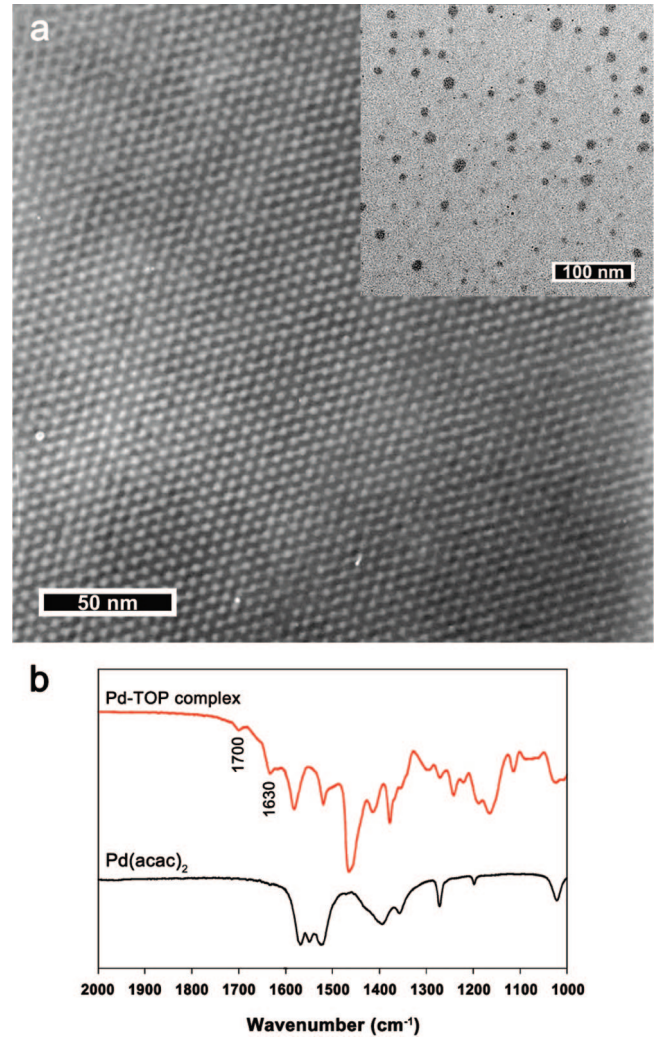

FIGURE 9. (a) TEM image of palladium nanoparticles in hexagonal superlattice. In the inset, palladium nanoparticles synthesized using TPP as the coordinating solvent are shown. (b) Fourier transform IR spectra of $Pd(acac)_2$ and Pd−TOP complex. The complex was prepared by mixing $Pd(acac)_2$ and TOP. The peaks at 1630 and 1700 cm^{-1} are attributed to C=C and C=O bondings, respectively, in acetylacetonate groups in monodentate mode.

tion of Pd^{2+}. In addition, when oleylamine is added to the reaction mixture, the amine reduction route might be operational ($Pd^{2+} + 2NR_3 \rightarrow Pd^0 + 2NR_3^{+\bullet}$).[31] Second, the formation of the nanoparticles occurs at quite a high temperature. It has been reported that palladium nanoparticles can be produced well below 200 °C from the reaction of $Pd(acac)_2$ in various organic solvents such as methyl isobutyl ketone and xylenes.[32] In contrast, almost no nanoparticles were generated up to 215 °C in our synthesis using TOPO as a solvent. In a control experiment using triphenylphosphine [TPP] as the coordinating solvent, which has stronger binding ability for palladium nanoparticles than TOP, polydisperse nanoparticles were obtained (the inset of Figure 9a).[33] These results suggest that the presence of the coordinating solvent retards the formation of the nanoparticles at high temperature and that the optimal binding ability is critical for the formation of uniformly sized nanoparticles.

Our synthetic method for palladium nanoparticles was successfully applied to the synthesis of nanoparticles of copper and nickel using metal(II) acetylacetonates as the precursors (Figure 10a).[34,35] Our group further extended this route and was able to synthesize Ni/Pd core/shell nanoparticles. Inspired

SCHEME 4

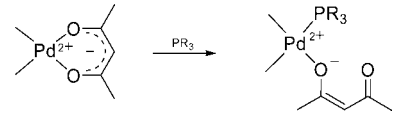

by our observation that nickel acetylacetonate decomposes at a significantly lower temperature than palladium acetylacetonate, we were able to synthesize Ni/Pd core/shell nanoparticles by simply heating the reaction mixture composed of acetylacetonates of nickel and palladium (Figure 10b).[33] During the heating process, the nickel-rich core forms at ~205 °C and the palladium-rich shell forms at 235 °C. This method highly simplifies the procedure for the synthesis of core/shell nanoparticles.

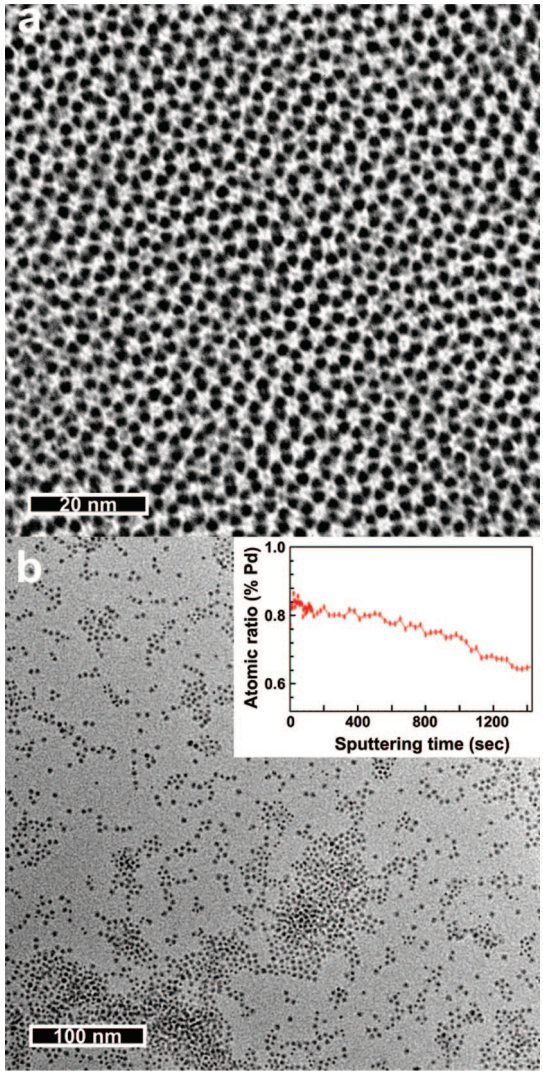

FIGURE 10. TEM image of (a) nickel nanoparticles in hexagonal superlattice and (b) Ni/Pd core/shell nanoparticles. In the inset, the depth profile of the atomic concentration of Pd measured with field-emission Auger electron spectroscopy is shown. According to elemental analysis on the same sample, the atomic ratio of Pd and Ni in bulk is 0.43/0.57.

V. Synthesis of Nanocrystals of Metal Chalcogenides Using Alternative Chalcogen Precursors

In the synthesis of metal chalcogenide nanocrystals, chalcogens are generally introduced in two ways. First, single-source precursors containing metal−chalcogen bonds such as metal xanthates [$M(S_2COR)_x$] are used. Second, chalcogen precursors such as trioctylphosphine chalcogenides (TOPSe and TOPTe) are reacted with metal precursors. The role of the precursors in the nanocrystal synthesis is very important because they greatly affect the synthetic conditions and the products. We synthesized uniform nanocrystals of various metal chalcogenides using alternative chalcogen reagents.

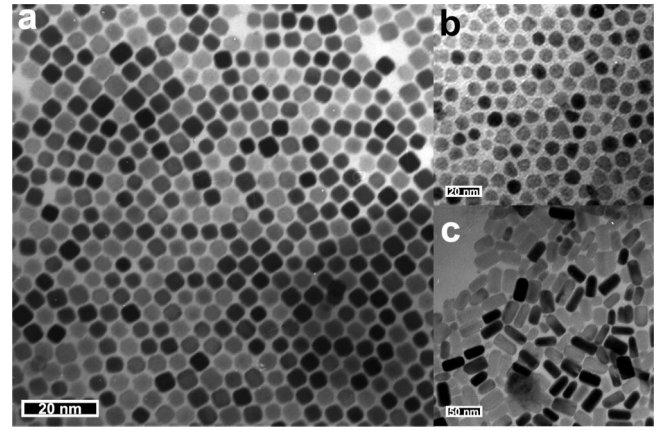

FIGURE 11. TEM images of (a) PbS, (b) ZnS, and (c) MnS nanocrystals.

SCHEME 5

$$RNH_2 + S_x \longrightarrow RN^+H_2{-}S_x^-$$

SCHEME 6

$$2RNH_2 + Se + CO \longrightarrow (RNH_3)^+(RHN{-}\overset{\overset{O}{\|}}{C}{-}Se)^-$$

In 2003, we introduced a general synthetic method for metal sulfide nanocrystals.[36] In the synthesis, metal chloride dissolved in oleylamine is reacted with the sulfur precursor under heating. The sulfur precursor is prepared by mixing elemental sulfur and oleylamine. This method has been successfully applied for the synthesis of uniform nanocrystals of PbS, ZnS, CdS, and MnS (Figure 11). The crystallization yield varies from 0.28 for ZnS to 0.77 for CdS. In general, metal chlorides and elemental sulfur are not reactive enough to produce nanocrystals. However, when combined with an amine, nanocrystals of metal sulfides can be produced at temperatures as low as 140 °C in the case of CdS nanocrystals. We think that an amine−sulfur compound containing a reactive Lewis basic sulfur group, which is generated from the reaction of amine and sulfur, is responsible for the high reactivity (Scheme 5).[37]

The discovery of this highly reactive amine−sulfur compound inspired us to develop other reactive chalcogen precursors for low-temperature reactions. We were able to synthesize selenocarbamate by bubbling CO gas into a mixture composed of selenium powder and octylamine at room temperature (Scheme 6).[38] From the reaction of this selenocarbamate with cadmium(II) chloride dissolved in octylamine at temperatures as low as 70 °C, we synthesized free-standing nanoribbons with a uniform thickness of 1.4 nm (Figure 12a−e) with the crystallization yield of 0.76.[39] Very interestingly, these ultrathin CdSe nanoribbons with two-dimensional quantum-confined structure exhibited an extremely narrow photoluminescence band (Figure 12f).

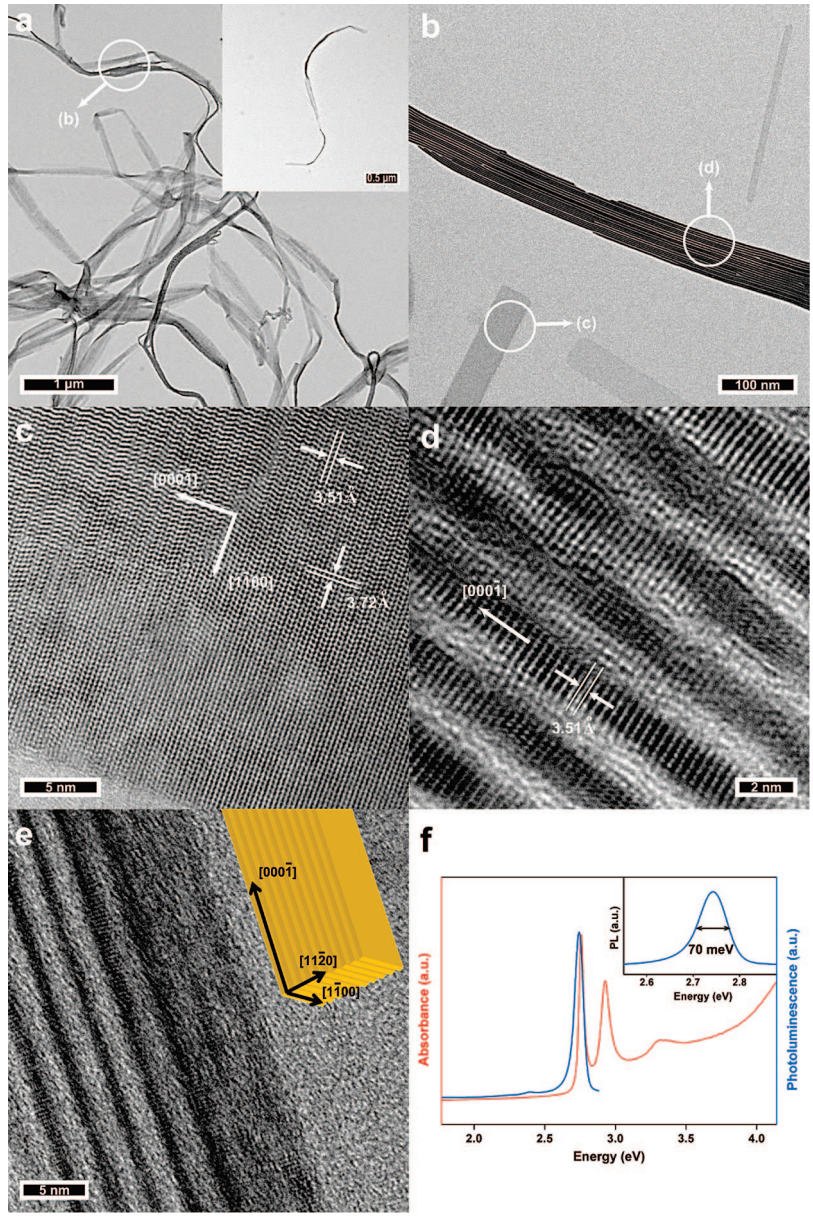

FIGURE 12. (a–e) TEM images of CdSe nanoribbons at various magnifications and (f) absorption and photoluminescence (PL) spectra of CdSe nanoribbons.

During the study of the synthetic process, we identified two critical factors for the formation of the nanoribbons, the reaction temperature and the steric effect of the coordinating solvent. When the reaction temperature was increased above 100 °C, a mixture composed of only polydisperse tetrapods and nanorods was generated, which demonstrates that the high thermal energy disturbs the anisotropic growth habit of the CdSe nanocrystals. In a series of control experiments using primary amines with various alkyl chain lengths, we found that the presence of an amine with an optimal chain length is critical for the synthesis of the nanoribbons. The two factors described above are satisfied with the use of octylselenocarbamate as the selenium precursor, which shows clearly the importance of the precursor in the designed synthesis of nanocrystals.

VI. Conclusion and Outlook

In this Account, we described the synthesis of uniformly sized nanocrystals using four different synthetic approaches including thermal decomposition, nonhydrolytic sol–gel reactions, thermal reduction, and reactions with reactive chalcogen precursors. Using these four kinds of synthetic processes, we were able to synthesize uniform nanocrystals of metals, oxides, and chalcogenides having various shapes. The overall process of the size distribution control of the thermal decomposition

method consists of three steps: the formation and accumulation of monomers, burst nucleation, and diffusion-controlled growth for size focusing, which fit very well to the LaMer model for the formation of monodisperse particles. The synthetic procedures summarized in this Account are highly reproducible and readily applicable for the large-scale synthesis of uniformly sized nanocrystals.

In the future, obtaining a detailed understanding of nanocrystal formation kinetics and synthetic chemistry will lead to the synthesis of uniform nanocrystals with controlled size, shape, and composition. In particular, the synthesis of uniform nanocrystals of doped materials, core/shell materials, and multicomponent materials is still very much a challenge. We expect that many of these uniformly sized nanocrystals will find numerous important applications in various areas including information technology, biomedical areas, and energy/environmental technology.

We would like to thank the Korean Ministry of Education, Science and Technology for the funding through the National Creative Research Initiative Program of the Korea Science and Engineering Foundation (KOSEF).

BIOGRAPHICAL INFORMATION

Soon Gu Kwon received his B.S. (2004) from the School of Chemical and Biological Engineering of the Seoul National University. He is now in the Ph.D. course under the supervision of Prof. Taeghwan Hyeon. His research interests are focused on the synthesis of nanocrystals and the formation mechanism of monodisperse nanocrystals.

Taeghwan Hyeon received his B.S. (1987) and M.S. (1989) in Chemistry from the Seoul National University, Korea. He obtained his Ph.D. in Chemistry from the University of Illinois at Urbana−Champaign (1996). Since he joined the faculty of the School of Chemical and Biological Engineering of Seoul National University in September 1997, he has been focused on the synthesis and applications of uniformly sized nanocrystals and nanoporous carbon materials, and he has published more than 110 papers in prominent international journals. He is currently Director of National Creative Research Initiative Center for Oxide Nanocrystalline Materials supported by the Korean Ministry of Education, Science and Technology. He is currently serving as editorial board member of *Advanced Materials*, *Small*, *Chemical Communications*, and *International Journal of Nanotechnology*.

FOOTNOTES

*To whom correspondence should be addressed. E-mail: thyeon@snu.ac.kr. Tel: 82-2-880-7150. Fax: 82-2-886-8457.

REFERENCES

1 Park, J.; Joo, J.; Kwon, S. G.; Jang, Y.; Hyeon, T. Synthesis of Monodisperse Spherical Nanocrystals. *Angew. Chem., Int. Ed.* **2007**, *46*, 4630–4660.

2 El-Sayed, M. A. Small Is Different: Shape-, Size-, and Composition-Dependent Properties of Some Colloidal Semiconductor Nanocrystals. *Acc. Chem. Res.* **2004**, *37*, 326–333.

3 Klimov, V. I., Ed. *Semiconductor and Metal Nanocrystals*; Marcel Dekker, Inc.: New York, 2004.

4 Murray, C. B.; Norris, D. J.; Bawendi, M. G. Synthesis and Characterization of Nearly Monodisperse CdE(E=S, Se, Te) Semiconductor Nanocrystallites. *J. Am. Chem. Soc.* **1993**, *115*, 8706–8715.

5 Peng, X.; Wickham, J.; Alivisatos, A. P. Kinetics of II-VI and III-V Colloidal Semiconductor Nanocrystal Growth: "Focusing" of Size Distributions. *J. Am. Chem. Soc.* **1998**, *120*, 5343–5344.

6 Donegá, C. d. M.; Liljeroth, P.; Vanmaekelbergh, D. Physicochemical Evaluation of the Hot-Injection Method, a Synthesis Route for Monodisperse Nanocrystals. *Small* **2005**, *1*, 1152–1162.

7 Sun, S.; Murray, C. B.; Weller, D.; Folks, L.; Moser, A. Monodisperse FePt Nanoparticles and Ferromagnetic FePt Nanocrystal Superlattices. *Science* **2000**, *287*, 1989–1992.

8 Na, H. B.; Lee, J. H.; An, K.; Park, Y. I.; Park, M.; Lee, I. S.; Nam, D. H.; Kim, S. T.; Kim, S. H.; Kim, S. W.; Lim, K. H.; Kim, K. S.; Kim, S. O.; Hyeon, T. Development of a T_1 Contrast Agent for Magnetic Resonance Imaging Using MnO Nanoparticles. *Angew. Chem., Int. Ed.* **2007**, *46*, 5397–5401.

9 Park, S. J.; Kim, S.; Lee, S.; Khim, Z. G.; Char, K.; Hyeon, T. Synthesis and Magnetic Studies of Uniform Iron Nanorods and Nanospheres. *J. Am. Chem. Soc.* **2000**, *122*, 8581–8582.

10 Hyeon, T.; Lee, S. S.; Park, J.; Chung, Y.; Na, H. B. Synthesis of Highly Crystalline and Monodisperse Maghemite Nanocrystallites without a Size-Selection Process. *J. Am. Chem. Soc.* **2001**, *123*, 12798–12801.

11 Park, J.; Lee, E.; Hwang, N. M.; Kang, M.; Kim, S. C.; Hwang, Y.; Park, J. G.; Noh, H. J.; Kim, J. Y.; Park, J. H.; Hyeon, T. One-Nanometer-Scale Size-Controlled Synthesis of Monodisperse Magnetic Iron Oxide Nanoparticles. *Angew. Chem., Int. Ed.* **2005**, *44*, 2872–2877.

12 Wonterghem, J. v.; Mørup, S.; Charles, S. W.; Wells, S. An Investigation of the Chemical Reactions Leading to the Formation of Ultrafine Amorphous $Fe_{100-x}C_x$ Alloy Particles. *J. Colloid Interface Sci.* **1988**, *121*, 558–563.

13 Casula, M. F.; Jun, Y.-w.; Zaziski, D. J.; Chan, E. M.; Corrias, A.; Alivisatos, A. P. The Concept of Delayed Nucleation in Nanocrystal Growth Demonstrated for the Case of Iron Oxide Nanodisks. *J. Am. Chem. Soc.* **2006**, *128*, 1675–1682.

14 Hyeon, T.; Chung, Y.; Park, J.; Lee, S. S.; Kim, Y. W.; Park, B. H. Synthesis of Highly Crystalline and Monodisperse Cobalt Ferrite Nanocrystals. *J. Phys. Chem. B* **2002**, *106*, 6831–6833.

15 Kang, E.; Park, J.; Hwang, Y.; Kang, M.; Park, J. G.; Hyeon, T. Direct Synthesis of Highly Crystalline and Monodisperse Manganese Ferrite Nanocrystals. *J. Phys. Chem. B* **2004**, *108*, 13932–13935.

16 Park, J.; An, K.; Hwang, Y.; Park, J. G.; Noh, H. J.; Kim, J. Y.; Park, J. H.; Hwang, N. M.; Hyeon, T. Ultra-Large-Scale Syntheses of Monodisperse Nanocrystals. *Nat. Mater.* **2004**, *3*, 891–895.

17 Choi, S. H.; Kim, E. G.; Park, J.; An, K.; Lee, N.; Kim, S. C.; Hyeon, T. Large-Scale Synthesis of Hexagonal Pyramid-Shaped ZnO Nanocrystals from Thermolysis of Zn-Oleate Complex. *J. Phys. Chem. B* **2005**, *109*, 14792–14794.

18 An, K.; Lee, N.; Park, J.; Kim, S. C.; Hwang, Y.; Park, J. G.; Kim, J. Y.; Park, J. H.; Han, M. J.; Yu, J.; Hyeon, T. Synthesis, Characterization, and Self-Assembly of Pencil-Shaped CoO Nanorods. *J. Am. Chem. Soc.* **2006**, *128*, 9753–9760.

19 Kim, D.; Park, J.; An, K.; Yang, N. K.; Park, J. G.; Hyeon, T. Synthesis of Hollow Iron Nanoframes. *J. Am. Chem. Soc.* **2007**, *129*, 5812–5813.

20 Kwon, S. G.; Piao, Y.; Park, J.; Angappane, S.; Jo, Y.; Hwang, N. M.; Park, J. G.; Hyeon, T. Kinetics of Monodisperse Iron Oxide Nanocrystal Formation by Heating-Up Process. *J. Am. Chem. Soc.* **2007**, *129*, 12571–12584.

21 Talapin, D. V.; Rogach, A. L.; Haase, M.; Weller, H. Evolution of an Ensemble of Nanoparticles in a Colloidal Solution: Theoretical Study. *J. Phys. Chem. B* **2001**, *105*, 12278–12285.

22 Sugimoto, T. Preparation of Monodisperse Colloidal Particles. *Adv. Colloid Interfac. Sci.* **1987**, *28*, 65–108.

23 Brinker, C. J.; Scherer, G. W. *Sol-Gel Science*; Academic Press: Boston, 1990.

24 Vioux, A. Nonhydrolytic Sol−Gel Routes to Oxides. *Chem. Mater.* **1997**, *9*, 2292–2299.

25 Niederberger, M. Nonaqueous Sol−Gel Routes to Metal Oxide Nanoparticles. *Acc. Chem. Res.* **2007**, *40*, 793–800.

26 Joo, J.; Yu, T.; Kim, Y. W.; Park, H. M.; Wu, F.; Zhang, J. Z.; Hyeon, T. Multigram Scale Synthesis and Characterization of Monodisperse Tetragonal Zirconia Nanocrystals. *J. Am. Chem. Soc.* **2003**, *125*, 6553–6557.

27 Trentler, T. J.; Denler, T. E.; Bertone, J. F.; Agrawal, A.; Colvin, V. L. Synthesis of TiO_2 Nanocrystals by Nonhydrolytic Solution-Based Reactions. *J. Am. Chem. Soc.* **1999**, *121*, 1613–1614.

28 Joo, J.; Kwon, S. G.; Yu, J. H.; Hyeon, T. Synthesis of ZnO Nanocrystals with Cone, Hexagonal Cone, and Rod Shapes via Non-Hydrolytic Ester Elimination Sol-Gel Reactions. *Adv. Mater.* **2005**, *17*, 1873–1877.

29 Joo, J.; Kwon, S. G.; Yu, T.; Cho, M.; Lee, J.; Yoon, J.; Hyeon, T. Large-Scale Synthesis of TiO_2 Nanorods via Nonhydrolytic Sol−Gel Ester Elimination Reaction and Their Application to Photocatalytic Inactivation of *E. coli*. *J. Phys. Chem. B* **2005**, *109*, 15297–15302.

30 Kim, S. W.; Park, J.; Jang, Y.; Chung, Y.; Hwang, S.; Hyeon, T.; Kim, Y. W. Synthesis of Monodisperse Palladium Nanoparticles. *Nano Lett.* **2003**, *3*, 1289–1291.

31 Blanchard, G. J.; Newman, J. D. S. Formation of Gold Nanoparticles Using Amine Reducing Agents. *Langmuir* **2006**, *22*, 5882–5887.

32 Esumi, K.; Tano, T.; Meguro, K. Preparation of Organopalladium Particles from Thermal Decomposition of Its Organic Complex in Organic Solvents. *Langmuir* **1989**, *5*, 268–270.

33 Son, S. U.; Jang, Y.; Park, J.; Na, H. B.; Park, H. M.; Yun, H. J.; Lee, J.; Hyeon, T. Designed Synthesis of Atom-Economical Pd/Ni Bimetallic Nanoparticle-Based Catalysts for Sonogashira Coupling Reactions. *J. Am. Chem. Soc.* **2004**, *126*, 5026–5027.

34 Son, S. U.; Park, I. K.; Park, J.; Hyeon, T. Synthesis of Cu_2O Coated Cu Nanoparticles and Their Successful Applications to Ullmann-Type Amination Coupling Reactions of Aryl Chlorides. *Chem. Commun.* **2004**, *778*, 779.

35 Park, J.; Kang, E.; Son, S. U.; Park, H. M.; Lee, M. K.; Kim, J.; Kim, K. W.; Noh, H. J.; Park, J. H.; Bae, C. J.; Park, J. G.; Hyeon, T. Monodisperse Nanoparticles of Ni and NiO: Synthesis, Characterization, Self-Assembled Superlattices, and Catalytic Applications in the Suzuki Coupling Reaction. *Adv. Mater.* **2005**, *17*, 429–434.

36 Joo, J.; Na, H. B.; Yu, T.; Yu, J. H.; Kim, Y. W.; Wu, F.; Zhang, J. Z.; Hyeon, T. Generalized and Facile Synthesis of Semiconducting Metal Sulfide Nanocrystals. *J. Am. Chem. Soc.* **2003**, *125*, 11100–11105.

37 Davis, R. E.; Nakshbendi, H. F. Sulfur in Amine Solvents. *J. Am. Chem. Soc.* **1962**, *84*, 2085–2090.

38 Sonoda, N.; Yasuhara, T.; Kondo, K.; Ikeda, T.; Tsutsumi, S. A New Synthesis of Ureas. The Reaction of Ammonia or Aliphatic Amines with Carbon Monoxide in the Presence of Selenium. *J. Am. Chem. Soc.* **1971**, *93*, 6344.

39 Joo, J.; Son, J. S.; Kwon, S. G.; Yu, J. H.; Hyeon, T. Low-Temperature Solution-Phase Synthesis of Quantum Well Structured CdSe Nanoribbons. *J. Am. Chem. Soc.* **2006**, *128*, 5632–5633.